Available online at www.sciencedirect.com
SCIENCE DIRECT®
ELSEVIER
Nuclear Instruments and Methods in Physics Research B xxx (2005) xxx–xxx
NIM B
Beam Interactions with Materials & Atoms
www.elsevier.com/locate/nimb

New program to estimate layer thicknesses from CEMS spectra

Ferenc Nagy [a,*], Zoltán Klencsár [b]

[a] Chemical Research Center, Department of Nuclear Chemistry, Eötvös Loránd University, Pázmány Péter sétány 1/A, Budapest 1117, Hungary
[b] Department of Applied Mathematics and Physics, University of Kaposvár, Guba Sándor u. 40, Kaposvár 7400, Hungary

Received 8 September 2005
Available online

Abstract

A new program, named BEATRICE, has been developed for the quantitative estimation of layer thicknesses of single- and multilayers on the basis of their CEMS (conversion electron Mössbauer spectroscopy) spectra. The BEATRICE program is able to estimate the individual layer thicknesses of multilayers consisting of several homogeneous or mixed nanolayers. The program can also be applied for samples with composition varying continuously with depth, as well as for samples displaying columns of different layer structures. The capability of the program is demonstrated by deriving functional dependences between relative CEMS subspectrum areas and sublayer thicknesses in simple but practically important cases.

PACS: 33.45.+x; 82.80.Ej; 87.64.Pj; 68.55.–a; 68.55.Jk; 68.55.Nq

Keywords: Multilayers; Mössbauer spectroscopy; CEMS

1. Introduction

The emerging role of thin layers in diverse fields of physics, chemistry, electronics and other industries raises the need for quantitative characterization methods sensitive to the composition of thin (with thickness in the nm to μm range) surface layers of bulk materials. One of the methods that can provide valuable information on the composition details of thin surface layers is conversion electron Mössbauer spectroscopy (CEMS). The CEMS method is applicable to surfaces containing Mössbauer active elements such as ^{57}Fe and ^{119}Sn. The method can be used most advantageously in the case of the qualitative and quantitative analysis of iron containing surface layers (about 2.14% of all the iron nuclei is Mössbauer active ^{57}Fe in natural iron). However, while CEMS spectra can often immediately inform about the qualitative composition of a surface layer (i.e. about the different types of phases and iron microenvironments), derivation of quantitative information (e.g. the concentration of different phases) requires further considerations assuming the knowledge of parameters (e.g. Mössbauer–Lamb factors characteristic of the different iron microenvironments, or the depth where the identified phases are situated in the surface) which are often not known with sufficient precision. Due to these difficulties, the application of CEMS is often restricted to the derivation of qualitative information only.

In this article we report about a newly developed computer program, named BEATRICE,[1] that is able to relate a high variety of surface structures and compositions to area ratios of subspectra expected in a CEMS spectrum taken from a surface layer with the corresponding structure and composition. By providing tools for adjusting continuously varying parameters of structure and composition (e.g. layer thicknesses and concentration parameters) to find the best

* Corresponding author. Tel.: +36 1 209 0593; fax: +36 1 209 0602.
E-mail address: nagyf@para.chem.elte.hu (F. Nagy).

[1] After Backward Estimation of lAyer Thicknesses from tRansmission Integrals of Conversion Electrons.

0168-583X/$ - see front matter © 2005 Published by Elsevier B.V.
doi:10.1016/j.nimb.2005.11.049

fit between the assumed quantitative properties of the surface layer and the experimentally observed CEMS spectrum, the program can be used efficiently to derive quantitative information from CEMS spectra.

2. Conversion electron Mössbauer spectroscopy (CEMS)

Under Mössbauer effect one means the recoilless nuclear resonance absorption of nuclear gamma radiation. During nuclear resonance absorption of nuclear gamma radiation a certain kind of nucleus (e.g. ^{57}Fe), being in the ground state, absorbs a gamma quantum emitted by a same kind of nucleus being in an excited state. The occurrence of such resonance absorption can be monitored in several different ways. In a transmission Mössbauer measurement the number of γ quanta *not* absorbed (i.e. transmitted) by the absorber is measured as a function of source velocity. In this case, at velocities where the condition of nuclear resonance absorption is fulfilled, a transmission minimum (i.e. an absorption peak) occurs. Other possibilities are the detection of secondary radiation emitted by the absorber as a result of the de-excitation of Mössbauer nuclei that were excited by the resonance absorption of γ quanta. This secondary radiation consists of reemitted γ quanta, conversion and Auger electrons, as well as characteristic X-rays. The detection of this secondary radiation in a Mössbauer experiment is called the scattering technique. In the field of surface layer studies, the most advantageous scattering technique is the one based on the detection of conversion electrons.

In conversion electron Mössbauer spectroscopy usually a proportional gas counter is used to detect conversion electrons back-scattered from the surface of the absorber sample (Fig. 1), and in contrast with the transmission technique, in the Mössbauer spectrum one observes maximal count rates whenever the condition of resonance absorption is fulfilled. As electrons originating deeper than a few 100 nm below the surface of the sample are very unlikely to be able to leave the sample and get counted, conversion electron Mössbauer spectroscopy is especially well suited to investigate this few 100 nm thick surface of solids.

The CEMS technique has the inherent advantage that the process of de-excitation of Mössbauer nuclei in the sample results in a high yield of conversion electrons for most of the practically important Mössbauer transitions. This is because of the high conversion coefficients ($\alpha = N_e/N_\gamma$) characteristic of low energy Mössbauer transitions. In the case of the 14.41 keV Mössbauer transition of ^{57}Fe, for example, $\alpha = 8.21$ meaning that in 89% of the cases de-excitation of corresponding excited state ^{57}Fe nuclei happens via the emission of a conversion electron.

The CEMS method found applications in various areas of scientific and industrial research [1]. Determination of the thickness and composition of corrosion layers [2], characterization of thin layers used for the passivation of iron [3], investigation of the magnetic structure of magnetic multilayers [4], and the study of the effect of ion implantation on the structure of surface layers [5–7] are a few characteristic examples.

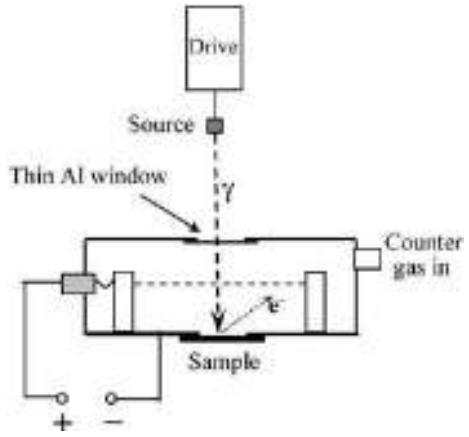

Fig. 1. Schematic representation of a conversion electron Mössbauer spectroscopy (CEMS) measurement. The γ quanta emitted by the source enter the volume of the proportional gas counter containing the counter gas (e.g. mixture of He + a few % CH_4) through a thin Al window. The sample is mounted on the detector such that its surface is directly in touch with the counting gas. Resonance absorption of γ quanta in the sample is followed by de-excitation of Mössbauer nuclei, as a result of which conversion- and corresponding Auger electrons enter the detector volume, and trigger an electronic impulse.

3. Observing quantitative information from CEMS spectra

Although by CEMS it is relatively easy to gain information concerning the kind of phases being present in a surface layer, the determination of the depth and the concentration of a particular phase require the detailed consideration of the interaction of electrons with matter. To estimate the weight of contribution of a particular phase to the CEMS spectrum, one has to know the probability of the event that electrons set free in that phase as a result of de-excitation of Mössbauer nuclei will reach the detector and gets counted. This probability will depend among others on the initial energy of the electron, on the depth of its origin, and on the kind of phases it has to pass through during its way to the top of the surface and the detector. For a certain surface layer, the function expressing the dependence of this probability on the depth of the origin of electrons is called the *transmission function*.

A conversion electron originating during de-excitation of a ^{57}Fe nucleus in the investigated sample is usually not the only electron leaving the corresponding atom as a result of the nuclear de-excitation process; the emission of a K-shell conversion electron can be followed also by the emission of corresponding Auger electrons. The emission probabilities of conversion- and various types of Auger electrons per nuclear de-excitation process are summarized in Table 1 (for ^{57}Fe) [8] and in Table 2 (for ^{119}Sn) [1].

Electrons traveling in different phases will experience a different rate of energy loss. The so-called *differential energy loss* of electrons, defined as the loss of electron

Table 1
Electron energies and conversion probabilities for ^{57}Fe [8]

Particle type	Origin	Probability per de-excitation	Initial energy
Electron	K conversion	$c_K = 0.80$	$E_K = 7.3$ keV
	L, M conversion	$c_L = 0.10$	$E_L = 13.6$ keV
	K Auger	$c_A = 0.53$	$E_A = 5.6$ keV

Table 2
Electron energies and conversion probabilities for ^{119}Sn [1]

Particle type	Origin	Probability per de-excitation	Initial energy
Electron	L conversion	$c_L = 0.84$	$E_L = 19.8$ keV
	L, N Auger	$c_A = 0.75$	$E_A = 2.8$ keV

kinetic energy on a path of unit length, is therefore a factor that strongly influences the magnitude and shape of the transmission function. First trials to calculate the differential energy loss function of electrons were carried out by Bethe [9]. Although electrons on their way to the surface are scattered (and may eventually even be stopped) via a series of elastic and inelastic collisions, and therefore loose their kinetic energy in several discrete amounts, the average loss of electron energy during this process can be approximated as a continuous energy loss. According to Joy and Luo [10] this energy loss can be written as

$$\frac{dE}{ds} = -78\,500\frac{Z}{AE}\ln\left(\frac{1.166E}{J}\right), \quad (1)$$

where E is the kinetic energy of the electron, s refers to the length of its path, Z is the atomic number, A is the mass number and J is the ionization energy of atoms building up the material. The ionization energy J also depends on the atomic number of atoms, which dependence can be estimated by the empirical formula

$$J/\text{eV} = 9.76Z + \frac{58.5}{Z^{0.19}}, \quad (2)$$

where Z denotes the atomic number of the atom in question [11].

The derivation of the escape probability of electrons as a function of their depth of origin, initial kinetic energy and the atomic number characteristic of the material layer they have to pass was carried out by Liljequist. By using established empirical relationships, like Eqs. (1) and (2), he made extensive Monte Carlo simulations by modeling the fate of individual electrons originating with different initial kinetic energies and traveling through materials with different characteristic atomic number [8,12–19]. By counting the number of electrons which in the simulation could reach the detector, Liljequist established empirical relationships between the escape probability of electrons and parameters such as the initial electron energy, the depth of origin and the atomic number of atoms in the surface layer [20].

One of the main conclusions of Liljequist's work is the so-called *mass scaling rule*, which states that the dependence of the transmission function on the atomic number characteristic of the surface layer to a high degree can be accounted for if the transmission probability is expressed as a function of the D surface density (also called *mass thickness*) measured in mass/area units. According to Liljequist [20,21], the transmission probability decreases with the D mass thickness as

$$T_1(D/R(E_i,Z)) = \exp\left[-\frac{D}{R(E_i,Z)} - \left(\frac{D}{Q\cdot R(E_i,Z)}\right)^2\right] = \exp\left[-\xi\left(1+\frac{\xi}{Q^2}\right)\right], \quad (3)$$

where $T_1(D/R(E_i, Z))$ is the probability that an electron born heading towards the top of the surface layer with initial kinetic energy E_i in a depth associated with mass thickness D, in a surface layer characterized by an atomic number Z will reach the top of the surface layer, $Q = 1.9$, $\xi = D/R(E_i, Z)$ and $R(E_i, Z)$ is a depth scale parameter (also called *Liljequist range*) which does not depend strongly on the atomic number, but it changes considerably with the electron's kinetic energy E_i. The dependence of $R(E_i, Z)$ on E_i and Z was also estimated on the basis of Monte Carlo simulations [20]:

$$\begin{aligned} R/\mu\text{g/cm}^2 &= \exp\left[\ln A + B\ln E_i + C(\ln E_i)^2\right],\\ A &= 2.630 + 4.03\times10^{-2}Z + 2.06\times10^{-4}Z^2,\\ B &= 1.660 - 1.63\times10^{-2}Z + 1.05\times10^{-4}Z^2,\\ C &= 0.034 + 2.00\times10^{-3}Z - 1.32\times10^{-5}Z^2, \end{aligned} \quad (4)$$

where E_i should be given in keV units.

Expression (3) is not the complete transmission function though, because it does not take into account that half of the electrons get born with a velocity that makes them to move *away* from the top of the layer surface initially. Still, such electrons may get scattered back towards the top of the surface (so-called *backscattering*), and therefore with a certain probability they will contribute to the number of escaped electrons. To obtain the correct expression for the transmission function T, T_1 must be multiplied by the factor $T_0(E_i, Z)$ that gives the transmission of those electrons that are born right on the surface of the sample (i.e. for which $\xi(E_i) = 0$) [20,21]:

$$T(D,E_i,Z) = T_0(E_i,Z)\cdot T_1(D/R(E_i,Z)) \quad (5)$$

with

$$T_0(E_i,Z) = 0.625 + 0.064\ln(Z/4) + 4.0\times10^{-6}Z^2 \times \ln(E_i/20\text{ keV}). \quad (6)$$

By substituting Eq. (6) into Eq. (5), for K conversion electrons born on the surface of, e.g. an alpha iron layer ($D = 0$, $Z \approx 26$, $E_i \approx 7.3$ keV, see Table 1), one observes a transmission of

$$T(D=0,E_i,Z)=T_0(E_i,Z)\approx 0.74. \quad (7)$$

The reason for not having obtained a transmission of unity for electrons born right on the surface of the sample is, certainly, that half of these electrons will have an initial propagation direction that points to the *inside* of the sample, and consequently they do not leave the sample surface immediately. The reason for not having obtained a transmission value of 0.5 is that a certain fraction of the latter electrons can still escape and get detected by being scattered back from the inside of the material. Detailed treatment of the backscattering process can be found, e.g. in [22,23].

For the case of a homogeneous alpha iron layer and initial electron energies encountered in ^{57}Fe CEMS measurements the dependence of the transmission function T on the D mass depth is displayed in Fig. 2. In accordance with expectations, with increasing D mass depth, among the detected electrons the share of electrons with higher initial energy will increase at the expense of the share of the lower energy electrons. As a result, in the case of ^{57}Fe CEMS, from depths with $D \gtrsim 160$ μg/cm^2 it will be almost exclusively the L, M conversion electrons (born with an initial energy of ~13.6 keV) that will be detected.

3.1. Handling of chemical compounds and their mixtures

The formulas discussed until this point are valid only for layers consisting only of a single type of element, i.e. iron in the case of ^{57}Fe CEMS, and tin in the case of ^{119}Sn CEMS. In practice, however, layers consist of several different elements that form different chemical compounds, which latter may furthermore be present combined forming mixtures of compounds. As the structure and composition of such layers is usually not known with sufficient precision on the atomic level, it seems to be unfeasible to derive a unique transmission function by Monte Carlo simulations for every layer encountered in practice. Thus, one has to find a way to estimate the transmission function for layers made of mixture of elements (which in the followings we will call as the '*compound transmission function*') on the basis of the transmission functions of layers built only from a single type of element. As relative area fractions of subspectra in a CEMS spectrum are determined usually with a relative error of higher than 1%, and relative errors of 10% are also not uncommon, our aim is to estimate compound transmission functions with a relative precision of $\lesssim 5\%$.

To achieve this goal, one has to investigate the dependence of the T_0 initial transmission function in Eq. (6) and that of the T_1 transmission function in Eq. (3) on the Z atomic number. At this point it should be noted, that unlike in Eq. (5) that is valid only for layers consisting only of a single type of element, in the case of compound layers, the parameter Z in $T_0(E_i, Z)$ and that in $T_1(D/R(E_i, Z))$ may not be the same. Namely, while the parameter Z in $T_1(D/R(E_i, Z))$ refers to the atomic number of elements situated between the point of origin of electrons and the top of the layer, the parameter Z appearing in $T_0(E_i, Z)$ (which factor takes the effect of backscattering into account) refers to the atomic number of elements below (in the sense 'farther away from the detector volume') the point of origin of electrons (Fig. 3).

Fig. 4 shows the dependence of the initial transmission $T_0(E_i, Z)$ on the layer's characteristic Z atomic number, for the E_i initial electron energies encountered in ^{57}Fe CEMS measurements. According to the figure, the initial transmission as a function of atomic number can be described nearly by the same curve for all the three different initial electron energies. The dependence of $T_0(E_i, Z)$ on Z is also rather mild; for atomic number values extending from $Z=2$ to $Z=80$ the value of initial transmission remains in the range 0.58–0.81. Even more importantly, $T_0(E_i, Z)$ is monotonously increasing as a function of Z. This suggests, that if we have a mixture of, e.g. two different elements (with atomic numbers $Z_1 < Z_2$) present in the

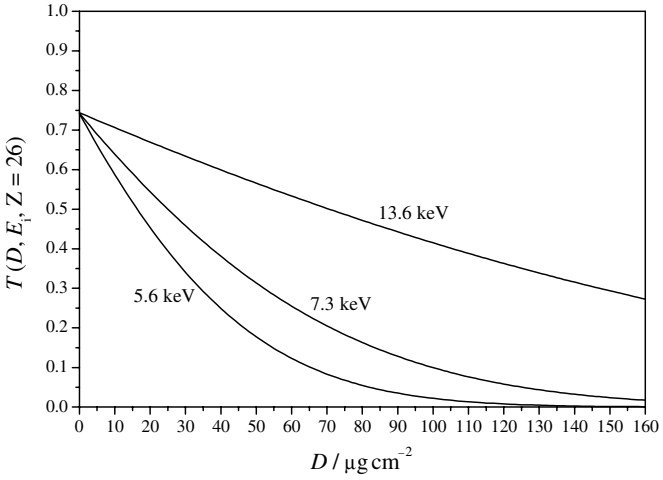

Fig. 2. The transmission function in Eq. (3) as a function of mass thickness D in the case of iron ($Z=26$) for the initial electron energies encountered in ^{57}Fe CEMS measurements (see also Table 1). For pure α-iron 10 μg/cm^2 mass thickness corresponds to a layer thickness of ~12.7 nm.

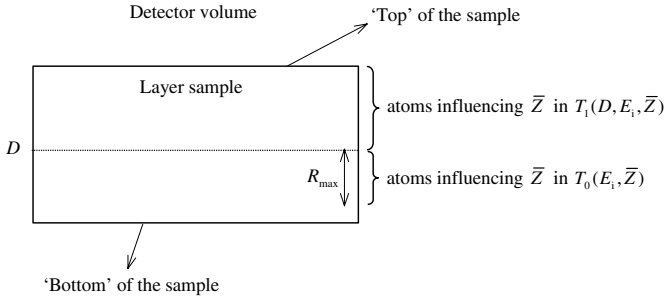

Fig. 3. At a certain D mass depth (denoted by dotted line) below the top of the surface of the investigated sample atoms influencing the $T_1(D/R(E_i, Z))$ transmission function in Eq. (3) are situated above the dotted line, while atoms that influence the $T_0(E_i, Z)$ initial transmission function (i.e. backscattering) are situated below the dotted line in a sublayer with a thickness of R_{max}, the maximum backscattering depth (see Eq. (11)).

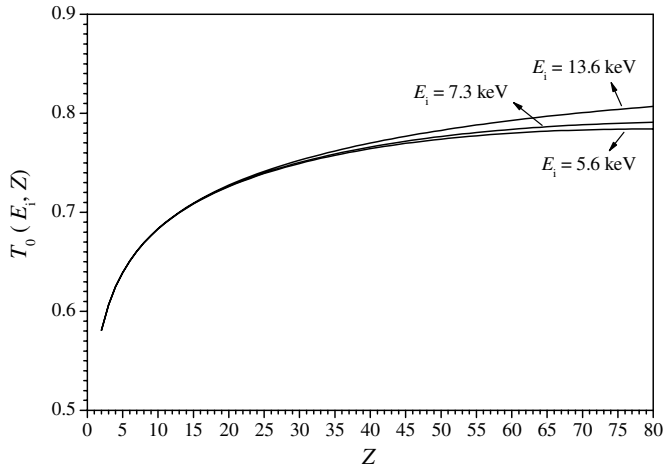

Fig. 4. The dependence of the initial transmission in Eq. (6) on the layer's characteristic Z atomic number, for the E_i initial electron energies encountered in ^{57}Fe CEMS measurements.

sample, then the value of the resulting '*compound initial transmission*' will be between the initial transmission value representative for Z_1 and that representative for Z_2, i.e.

$$T_0(E_i, Z_1) < T_{0c}(E_i, Z_1 \text{ and } Z_2) < T_0(E_i, Z_2) \quad (8)$$

if $Z_1 < Z_2$, where $T_{0c}(E_i, Z_1 \text{ and } Z_2)$ denotes the compound initial transmission. Also, one expects that with decreasing concentration of atoms with atomic number Z_1, the compound initial transmission will tend to approach the initial transmission value representative for the element with atomic number Z_2, and vice versa. This behavior suggests, that for compound samples we can define a certain kind of weighted average of atomic numbers, $\overline{Z}$, for which

$$T_{0c}(E_i, \text{ mixture of different elements}) \approx T_0(E_i, \overline{Z}), \quad (9)$$

in this way reducing the problem of the calculation of the compound transmission function to the problem of finding a suitable averaging method of atomic numbers that works well in practice. It was found, that the averaging method when the value of $\overline{Z}$ is calculated as an arithmetic average weighted by the w_i weight fractions of the atoms of different Z_i atomic numbers, i.e.

$$\overline{Z} = \sum_i w_i Z_i, \quad (10)$$

works well in practice [23], if as an exception among the elements hydrogen is taken into account with the 'effective' atomic number of $Z_{\text{eff}}(\text{H}) = -7.434$. The success of this averaging method means that for a given compound it is the heavier elements with the highest Z that predominantly determine the value of the initial transmission, though the presence of hydrogen can reduce the level of backscattering (see Fig. 4).

Before calculating $\overline{Z}$, one needs to determine the depth (below the point of origin of electrons) below which atoms should not be considered anymore when the average in Eq. (10) is calculated. According to Niedrig [22], this so-called '*maximum backscattering depth*' ($R_{\max}$) can be expressed as

$$R_{\max} = \frac{4E_i^2}{c_T \rho m_e^2}, \quad (11)$$

where E_i is the initial kinetic energy of electrons, ρ denotes the density of the sample material, m_e stands for the mass of the electron and $c_T = 5.05 \times 10^{33}\ \text{m}^6\ \text{kg}^{-1}\ \text{s}^{-4}$ is Terrill's constant. For our purposes it is more convenient to express the '*maximum backscattering mass depth*' ($B_{\max} = \rho R_{\max}$), which on the basis of Eq. (11) can be written as

$$B_{\max}\ [\mu\text{g/cm}^2] \approx 2.45 \times (E_i/\text{keV})^2. \quad (12)$$

As shown in Fig. 5, for ^{57}Fe CEMS the maximum backscattering mass depth is highest for the 13.6 keV L, M conversion electrons, for which it takes on a value of ~470 μg/cm^2. For pure α-iron this value corresponds to a layer thickness of ~600 nm. This means that for layers thinner than roughly this value the substrate material can also influence the backscattering process independent of the point of origin of the electrons, i.e. the same thin layer structure deposited on different substrates may result in different relative area ratios in the ^{57}Fe CEMS spectra, even if the substrates themselves do not contain any ^{57}Fe isotope. The effect of the substrate, however, becomes significant only for layers thinner than ~250 nm (see Fig. 2). Similar reasoning can be applied for the case of ^{119}Sn CEMS, where the maximum backscattering mass depth for the L conversion electrons is ~960 μg/cm^2 (Fig. 5), which is equivalent to a layer thickness of ~1315 nm for a pure tin layer.

Similarly to the initial transmission, in order to be able to predict relative CEMS spectrum areas as a function of layer structure, one also needs to give a useful estimate of the transmission function $T_1(D/R(E_i, Z)) \equiv T_1(D, E_i, Z)$ for compound materials. Following the same route of reasoning as before, we first investigate the dependence of $T_1(D, E_i, Z)$ on Z for different values of D and E_i. As

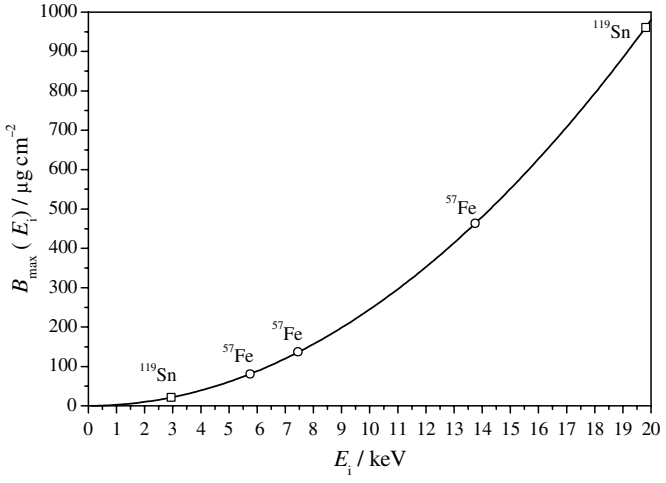

Fig. 5. The maximum backscattering mass depth, calculated according to Eq. (12), as a function of the electron's initial kinetic energy. Open circles and rectangles on the curve mark points with initial electron energy values encountered in ^{57}Fe and ^{119}Sn CEMS, respectively (see also Tables 1 and 2).

shown by Fig. 6, for E_i energies encountered in ^{57}Fe CEMS, in the practically important range of D mass depths $T_1(D, E_i, Z)$ has only a mild dependence on Z. Particularly, for $Z \leqslant 40$ the dependence of $T_1(D, E_i, Z)$ on Z is quite well approximated by a linear curve. But even if we extend the possible range of atomic numbers until $Z = 80$, and estimate $T_1(D, E_i, Z)$ by a constant for any given D and E_i value (i.e. we dismiss the Z dependence of $T_1(D, E_i, Z)$ altogether), the relative error we introduce into the end result by this approximation will still remain around or below ~5%. (Note that although the deviation of $T_1(D, E_i, Z)$ from the linear behavior becomes more pronounced with increasing D, the contribution of layers in different D mass depths to the total electron transmission also decreases with D, which effect for higher D values diminishes the higher error introduced by our approximation.) However, the linear dependence found for the case $Z \leqslant 40$ (which relation is expected to be satisfied for the majority of layers investigated in practice) suggests, that similarly to the case of the compound initial transmission $T_{0\ c}$ in Eq. (9), we should take the Z dependence of $T_1(D, E_i, Z)$ into account by defining the '*compound transmission function*' T_{1c} as

$$T_{1c}(D, E_i,\ \text{mixture of different elements}) \approx T_1(D, E_i, \overline{Z}), \tag{13}$$

where $\overline{Z}$ can be defined similarly to that in Eq. (10), where in the average one should consider only the part of the layer that is situated between the top of the layer and the point where the electron is set free.

By examining the dependence of $T_1(D, E_i, Z)$ on Z for initial electron energies encountered in ^{119}Sn CEMS (Fig. 7) one can conclude that for Auger electrons ($E_i = 2.8$ keV) the dependence is very well approximated by a linear curve, and therefore the aforementioned estimation of the compound transmission function by the calculation of an average atomic number may also work well in this case. The situation is different, however, in the case of the conversion electrons ($E_i = 19.8$ keV); for them the validity of linear approximation diminishes with increasing mass depth (see Fig. 7). For $D \gtrsim 200\ \mu g/cm^2$ one may consider to calculate an average atomic number independently for $Z \leqslant 50$ and $Z > 50$ elements, and estimate the T_{1c} compound transmission function as

$$T_{1c}(D, E_i,\ \text{mixture of different elements}) \approx \frac{T_1(D, E_i, \overline{Z}_{Z\leqslant 50}) + kT_1(D, E_i, \overline{Z}_{Z>50})}{1+k}, \tag{14}$$

where $\overline{Z}_{Z\leqslant 50}$ and $\overline{Z}_{Z>50}$ denote the weighted average of atomic numbers for those elements in the sample, for which $Z \leqslant 50$ and $Z > 50$, respectively, and $k \geqslant 0$ is a weight factor that takes into account the weight of elements with $Z > 50$ relative to that of elements with $Z \leqslant 50$.

From the compound functions T_{0c} and T_{1c} the electron transmission function can be calculated according to Eq. (5) as

$$T(D, E_i, Z^*) = T_{0c}(E_i,\ \text{mixture of different elements}) \cdot T_{1c}(D, E_i,\ \text{mixture of different elements}), \tag{15}$$

where the notation Z^* indicates that the dependence on Z is taken into account as described.

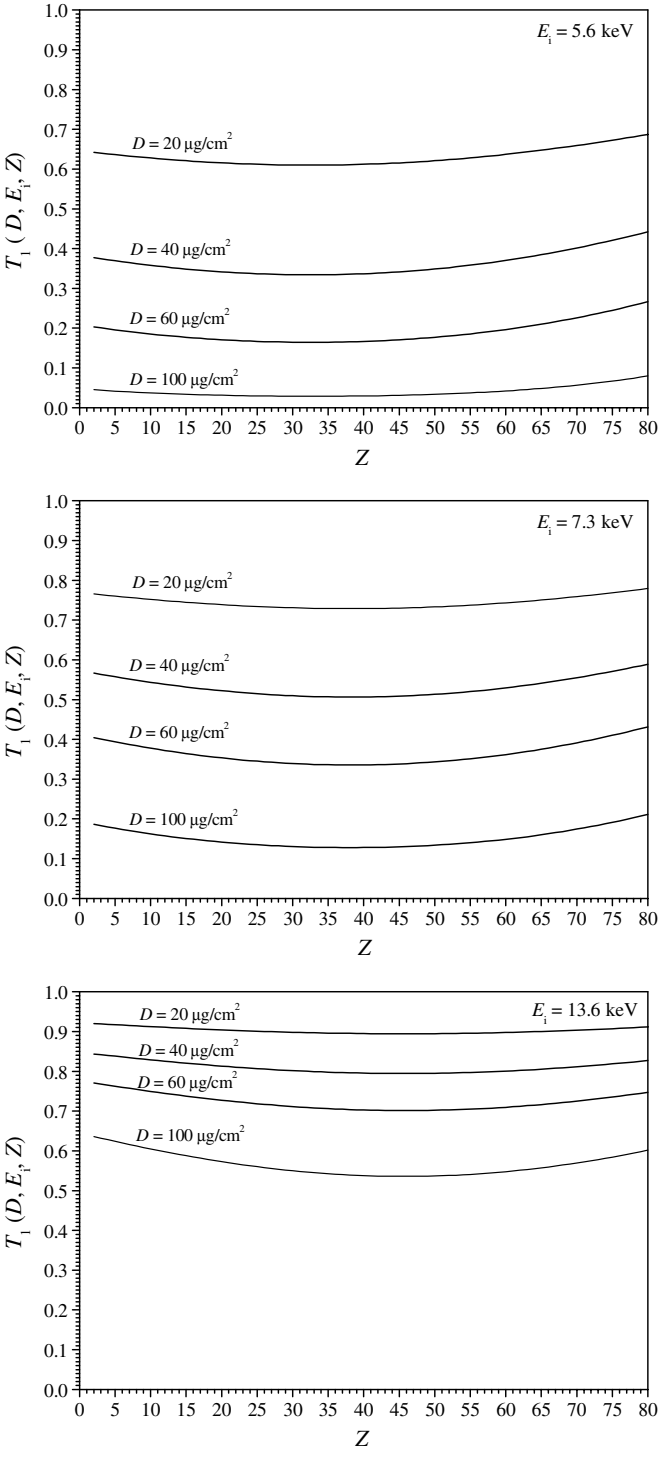

Fig. 6. The dependence of the transmission function T_1 in Eq. (3) on the layer's characteristic Z atomic number and on the mass depth where the electrons are born, for the E_i initial electron energies encountered in ^{57}Fe CEMS measurements.

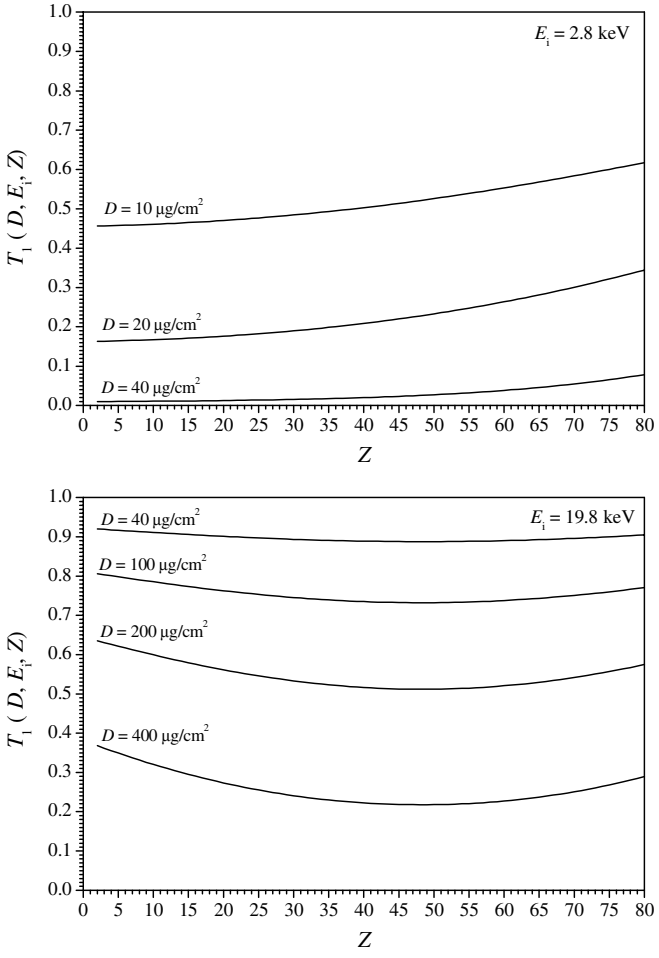

Fig. 7. The dependence of the transmission function T_1 in Eq. (3) on the layer's characteristic Z atomic number and on the mass depth where the electrons are born, for the E_i initial electron energies encountered in ^{119}Sn CEMS measurements.

Given that, according to the above, the dependence of the compound transmission function on the atomic number of elements building up the layer under study is relatively mild, one may presume, that the contribution of a certain phase to the CEMS spectrum will be determined first of all by the position (mass depth, D) of the phase inside the layer according to the dependence of the transmission function on D (Fig. 2). Different kind of phases may, however, still give different contributions to the CEMS spectrum, even if they are situated exactly at the same position inside the layer.

One reason for this can be that phases containing the Mössbauer active element (e.g. ^{57}Fe or ^{119}Sn) in higher concentrations will certainly produce a higher number of conversion and Auger electrons, consequently they will give a higher contribution to the CEMS spectrum if compared to phases with lower concentrations of the Mössbauer active element.

Another reason can be that different phases are usually characterized by different values of the so-called Mössbauer–Lamb factor, which latter is the probability of recoilless absorption of gamma rays by the Mössbauer active nucleus. A higher probability of recoilless absorption means a higher number of excited state Mössbauer nuclei, and consequently a higher number of conversion and Auger electrons originating during the de-excitation of these nuclei in the phase in question. Consequently, phases characterized by a higher Mössbauer–Lamb factor will have an increased contribution to the CEMS spectrum, if compared to the contribution of phases situated at the same position (same mass depth) in the layer but characterized by lower Mössbauer–Lamb factor values. It should be noted here, that if a phase contains the Mössbauer active element in two or more different microenvironments (as, e.g. in the case of Fe_3O_4, where there are two different iron microenvironments), then all the different microenvironments may be characterized by different Mössbauer–Lamb factor values. For such phases an $\bar{f}$ *effective Mössbauer–Lamb factor* may be defined as

$$\bar{f} = \frac{\sum_{i=1}^{n} k_i f_i}{\sum_{i=1}^{n} k_i}, \tag{16}$$

where n is the number of different iron microenvironments in the phase, k_i is the number and f_i is the Mössbauer–Lamb factor of iron atoms situated in the ith type of microenvironment.

3.2. The effective transmission

In order to calculate the expected contribution of Mössbauer active nuclei at a certain depth below the surface to the measured CEMS Mössbauer spectrum, one has to calculate the so-called *effective transmission*, which is the probability of the event that following a nuclear de-excitation process a corresponding electron will be detected by the detector. The effective transmission (T_e) of the electrons is calculated from the contribution of all the electrons with different energies, by taking into account their respective probabilities for being emitted as a result of a nuclear de-excitation process (Table 1), as well as the electron detection efficiency (ε) of the applied detector, which is here considered to be independent of the energy of the detected electron.

The probability of detection of electrons set free by the primary conversion process is given by

$$P_c = \varepsilon T(D, E_{i,c}, Z^*), \tag{17}$$

where $E_{i,c}$ denotes the initial energy of the primary conversion electron, and Z^* indicates that the dependence on Z should be taken into account as described in the previous section.

The primary (conversion) electron and the corresponding Auger electron(s) cannot be detected as separate events, because the finite, relatively long time duration of the detection process of the primary electron makes the detector deaf to the corresponding secondary (Auger) electrons [24]. An Auger electron leaving the atom shortly after the

conversion process has taken place can therefore be detected only if the conversion electron was not detected, i.e. the probability of detection of an Auger electron is given by

$$P_c = c_A T(D, E_{i,A}, Z^*)[1 - \varepsilon T(D, E_{i,c}, Z^*)], \quad (18)$$

where c_A is the probability that the Auger electron leaves the atom, $E_{i,A}$ is the Auger electron's initial energy and $T(D, E_{i,A}, Z^*)$ is the probability that the Auger electron reaches the detector.

By considering the K conversion, K Auger and L, M conversion electrons (Table 1) in the case of ^{57}Fe one observes an effective transmission of

$$T_e(D, Z^*) = \varepsilon[c_K T(D, E_K, Z^*) + c_A T(D, E_A, Z^*)(1 - \varepsilon T(D, E_K, Z^*)) + c_L T(D, E_L, Z^*)], \quad (19)$$

where the notations used are the same as in Table 1.

For the case of ^{119}Sn similar considerations lead to the effective transmission function of

$$T_e(D, Z^*) = \varepsilon[c_L T(D, E_L, Z^*) + c_A T(D, E_A, Z^*)(1 - \varepsilon T(D, E_L, Z^*))], \quad (20)$$

where the notations used are the same as in Table 2.

Given that the effective transmission decreases with the D mass depth, phases situated deeper than a so-called *visible mass depth* (D_v) will only give negligible contribution to the CEMS spectrum in the sense that their contribution will be below the detection limit of the CEMS method. If a phase provides only $\lesssim 1\%$ of all the detected electrons, then in most cases its contribution will remain hidden in the corresponding CEMS spectrum by the statistical noise of the measurement. Although in general the visible mass depth will depend on the structure of the investigated layer, a useful estimate of D_v can be calculated by assuming a homogeneous sample. For a homogeneous sample the relative amount of electrons (w) contributing to the CEMS spectrum from depths deeper than D_v can be expressed as

$$w = \frac{\int_{D_v}^{\infty} T_e(D, Z)\mathrm{d}D}{\int_0^{\infty} T_e(D, Z)\mathrm{d}D}, \quad (21)$$

which equation enables one to estimate the D_v visible mass depth on the basis of the value of w. For an α-iron layer, with the choice of $w = 0.01$ one observes a visible mass depth of $D_v \approx 340$ μg/cm^2, which is equivalent to a visible depth of ~432 nm. For a pure tin layer ($Z = 50$) for $w = 0.01$ one observes a visible mass depth of $D_v \approx 820$ μg/cm^2, which is equivalent to a visible depth of ~1123 nm. The value of the ε electron detection efficiency of the applied detector does not influence considerably the value of the D_v visible mass depth calculated according to Eq. (21).

3.3. Handling of multilayer structures

In practice, thin layers consisting of different phases (e.g. different corrosion products or electrochemically deposited layers) can often be satisfactorily modeled by a multilayer structure. In the multilayer the different phases are thought to form parallel sublayers as shown in case a, of Fig. 10. In the followings we aim to calculate the expected weight of contribution of the different phases of the multilayer to a corresponding CEMS spectrum.

Let us consider a sample consisting of N homogeneous layers made of different phases. Let the layers be numbered from layer $k = 1$ being on the surface to layer $k = N$ being the inner most Mössbauer active layer in the surface. In this case, the relative weight (S_k) by which layer k is expected to contribute to a CEMS spectrum can be expressed as

$$S_k = \frac{c_k f_k \int_{D_{k-1}}^{D_k} T_e(D, Z^*)\mathrm{d}D}{\sum_{j=1}^{N} c_j f_j \int_{D_{j-1}}^{D_j} T_e(D, Z^*)\mathrm{d}D} \quad (k = 1 \ldots N), \quad (22)$$

where c_k is the concentration of the Mössbauer active nuclide (e.g. ^{57}Fe) in layer k, f_k denotes the effective Mössbauer–Lamb factor characteristic of the phase in layer k, and

$$D_0 = 0, \quad D_k = D_{k-1} + m_k, \quad (23)$$

where m_k denotes the mass thickness of layer k. By using Eq. (22) the S_k values can be calculated for an arbitrary set of m_k mass thicknesses, c_k concentrations and f_k effective Mössbauer–Lamb factor values characteristic of the individual layers.

In practice, on the basis of the CEMS spectrum one usually can determine the type of phases that are present in the layer, which means that the concentrations and the corresponding effective Mössbauer–Lamb factors can be assumed to be known in the calculations. The order of the different sublayers is also often known (e.g. by studying the corrosion of an iron layer, one can often safely assume that corrosion products are at the top of the layer, and unaltered pure iron is situated at higher mass depths), or the possible number of different sublayer orders is small enough to make it feasible to try them out manually one by one, and select the one giving the best fit with the measured data. This means that in most cases it is only the D_k mass thicknesses of sublayers that are unknown and need to be determined by the help of fitting using an appropriate program code.

By comparing the S_k values – obtained according to Eq. (22) for a certain set of c_k concentrations and f_k effective Mössbauer–Lamb factor values – with the corresponding relative subspectrum areas of the experimentally measured CEMS spectrum, one can estimate the correct set of mass thicknesses by minimizing the squared differences between experimentally obtained and theoretically predicted relative subspectrum areas:

$$Y(m_1, m_2, \ldots, m_N) = \sum_{k=1}^{N} (A_k - S_k)^2 \Rightarrow \min, \quad (24)$$

where A_k denotes the relative area fraction of the subspectrum originating from sublayer k in the CEMS spectrum of the surface layer in question. From the obtained set of m_k mass thickness values and the ρ_k densities of the sublayer materials, the d_k layer thicknesses can be determined for each layer one by one.

The minimization problem of Eq. (24) involves N unknown parameters (the m_k mass thicknesses) to be fitted. In cases, however, when the total iron content of the layer is known the number of fitted parameters can be reduced by one by considering that the mass thicknesses of the individual sublayers have to satisfy the equation

$$\sum_{k=1}^{N} m_k w_k = \frac{M_{\mathrm{Fe}}}{F}, \tag{25}$$

where w_k is the weight fraction of iron in the kth layer, M_{Fe} is the total mass of iron in the layer, and F is the area of the layer's surface.

The considerations presented until this point form the basis of the BEATRICE program that is able to estimate the individual layer thicknesses of multilayers consisting of several homogeneous or mixed nanolayers. Apart from the determination of individual sublayer thicknesses by fitting according to Eq. (24), another possible way to use the program is to derive functional dependences between the expected CEMS relative subspectrum areas and the layer's characteristic physical parameters, e.g. sublayer thicknesses. The curves derived in this way may be used in practice to determine the physical parameters in question without the need for executing the fitting procedure of the program. The main advantage of the BEATRICE program is that it can handle a high variety of simple as well as complex practically important layer structures.

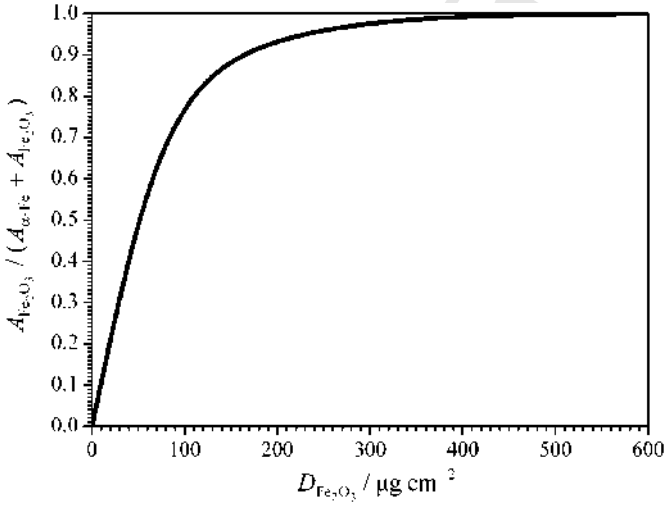

Fig. 8. The dependence of the relative CEMS spectral area of hematite on the mass thickness of hematite formed on the top of an infinitely thick (i.e. bulk) α-iron layer, as calculated by the BEATRICE program. $A_{\alpha\text{-Fe}}$ and $A_{Fe_2O_3}$ denote the CEMS spectral area belonging to α-Fe and hematite, respectively.

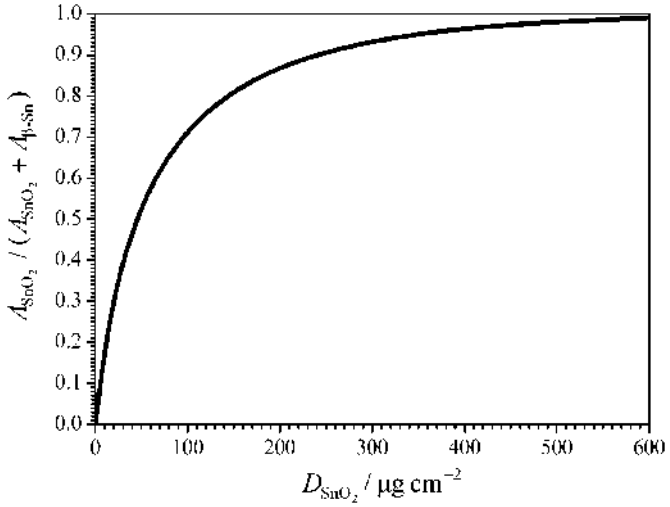

Fig. 9. The dependence of the relative CEMS spectral area of SnO_2 on the mass thickness of SnO_2 formed on the top of an infinitely thick (i.e. bulk) β-Sn layer, as calculated by the BEATRICE program. $A_{\beta\text{-Sn}}$ and A_{SnO_2} denote the CEMS spectral area belonging to β-Sn and SnO_2, respectively.

In order to demonstrate the program's capabilities, we derived the functional dependence between the mass thickness of an Fe_2O_3 layer formed by corrosion on the top of a thick (e.g. bulk, i.e. from our point of view infinitely thick) iron layer and the corresponding relative subspectrum area expected in a CEMS spectrum (Fig. 8). The relative spectral area belonging to the Fe_2O_3 layer increases nearly linearly with the mass thickness of Fe_2O_3 from $D_{Fe_2O_3} = 0\ \mu g/cm^2$ until $D_{Fe_2O_3} \approx 60\ \mu g/cm^2$. In this range, an increase of 10 μg/cm^2 in $D_{Fe_2O_3}$ results in an increase of ~0.1 in the relative spectral area of the Fe_2O_3 layer. The curve indicates that for above $D_{Fe_2O_3} \approx 200\ \mu g/cm^2$ the mass thickness of the hematite layer can be determined only with considerable uncertainty.

A similar curve is obtained for the case of SnO_2 formed on the top of a bulk β-Sn layer, as shown in Fig. 9.

4. Details of the BEATRICE program

Given that the majority of CEMS measurements are carried out on iron containing samples, the BEATRICE program treats ^{57}Fe as the default Mössbauer isotope. At the same time, the program provides the user with the possibility to override the default physical parameters in order to make the program handle Mössbauer isotopes other than ^{57}Fe. Among others the user can specify the probability of emission of K, L conversion electrons and Auger electrons per de-excitation, as well as their respective initial energies. One can furthermore set the electron pairs that hinder the detection of each other (see Section 3.2), in order to calculate the effective transmission analogously to Eqs. (19) and (20).

The program has a wired in set of physical parameters (atomic masses, molar volumes, Mössbauer–Lamb factors, etc.) concerning the most important iron compounds,

which set may be extended by the user for further compounds as needed.

The different surface layer structures that can be handled by the program can be summarized as follows.

A *simple set of sublayers* (case a, in Fig. 10) denotes layers that are built from sublayers that have ideally flat surfaces perpendicular to the main source – detector – carrier axis. The individual sublayers can be defined to be chemically homogeneous or a mixture of several different compounds. The order of sublayers from top to bottom of the layer needs to be defined in advance. The parameters to be determined by the program on the basis of the corresponding relative CEMS subspectrum areas are the mass thicknesses of the individual sublayers.

Multicolumn layers (see Fig. 11 and case d, in Fig. 10) denote columns of different sequences of sublayers, which structure aims to model samples where, for example, the top most sublayer does not cover entirely the surface of lower situated sublayers, which may happen e.g. when corrosion of an iron containing surface layer takes place in spots only. In such cases the underlying (not corroded) layers will display a contribution to the corresponding CEMS spectrum that is increased compared to the case of a continuous top most corrosion sublayer, because outside the spots electrons from the underlying layers will have an increased probability for detection. In the BETARICE program the case of multicolumn layers is reduced to a sum of several different simple set of sublayers as shown in Fig. 11. As this reduction is valid only if the diameter of the spots (columns) can be considered to be higher than the visible depth (otherwise the electrons could jump from one column to another), the model of multicolumn layers can be applied exclusively for such cases. The parameters to be determined by the program on the basis of the corresponding relative CEMS subspectrum areas in this case are the relative area fractions of the different columns as well as the mass thicknesses of the individual sublayers.

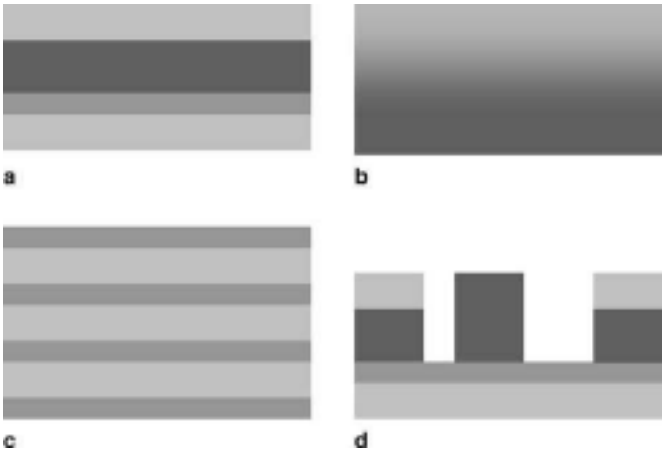

Fig. 10. Types of layer structures that can be handled by the BEATRICE program: (a) simple set of sublayers; (b) layers with continuously varying composition; (c) periodic layer structures; (d) layers with multicolumn surface structure.

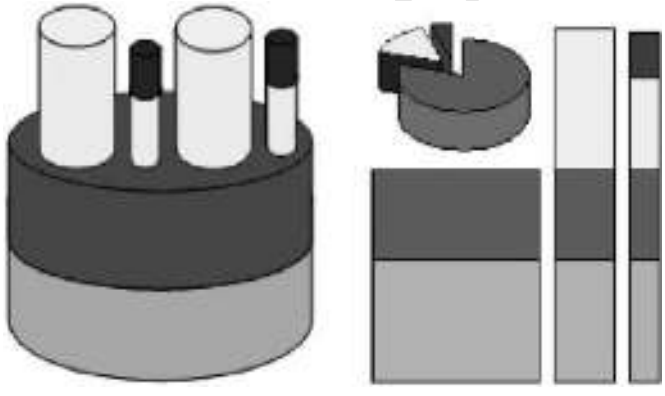

Fig. 11. Schematic representation of the way the BEATRICE program handles multicolumn layer structures. The multicolumn surface structure displayed on the left side of the figure can be treated as the sum of three different layers; one with two, one with three and a third with four sublayers, as shown on the right hand side of the figure.

In order to be able to model effects like diffusion for example, the program allows the definition of *depth dependent weight fractions* of components within sublayers (case b, in Fig. 10). The depth dependence can be defined by selecting one of the built in "relative sublayer depth → weight fraction" profiles. The program also allows the modeling of periodic sequences of sublayer compositions (case c, in Fig. 10).

The program can also handle user defined linear equality and inequality constraints among parameters (including the setting of the upper and lower bound of the various parameters).

Any user defined input data determining the model of the layer can be collected in an ASCII file in a specific tabular form, which file is then interpreted by the BEATRICE program before the corresponding calculations start, or alternatively the data can also be typed in by the help of the interactive command line input system the program offers.

The BEATRICE program was developed under MS Windows XP OS by using Fortran programming language and the programming environment Fortran Power Station 4.0. The program utilizes mathematical routines included in the IMSL Fortran Library [25]. Further information on the technical details of the BEATRICE program can be found on the WEB site http://www.chem.elte.hu/departments/magkem/nagyf/public_html/Angol/Beatrice.htm.

5. Conclusions

In order to calculate expected relative subspectrum areas in CEMS spectra of thin surface layers, the newly developed program named BEATRICE utilizes the electron transmission and backscattering functions obtained earlier as a result of Monte Carlo modeling of the fate of electrons with different energies in materials with different atomic numbers. By applying an appropriately chosen averaging method of the atomic numbers, the program was prepared

to handle layers made of compounds. To be able to model samples encountered in practice, the program was made ready to handle layers consisting of several different sublayers, layers with a columnar structure and layers with continuously varying depth dependent composition. With the tools it offers the BEATRICE program promotes the derivation of quantitative information from CEMS spectra recorded by the utilization of the Mössbauer effect of ^{57}Fe as well as other Mössbauer isotopes.

Acknowledgement

The authors are thankful to Prof. D. Liljequist for his helpful comments concerning the article.

References

[1] K. Nomura, Y. Ujihira, A. Vértes, J. Radioanal. Nucl. Chem. 202 (1996) 103.
[2] A. Vértes, Gy. Vankó, Z. Németh, Z. Klencsár, E. Kuzmann, Z. Homonnay, F.H. Kármán, E. Szöcs, E. Kálmán, Langmuir 18 (2002) 1206.
[3] Zs. Kajcsos, W. Meisel, E. Kuzmann, C. Tosello, M.L. Gratton, A. Vértes, P. Gütlich, D.L. Nagy, Hyp. Int. 57 (1990) 1883.
[4] U. Gradmann, J. Magn. Mater. 100 (1991) 484.
[5] G. Langouche, Hyp. Int. 45 (1989) 199.
[6] K.P. Mitrofanov, V.S. Shpinel, Soviet Phys. JETP13 (1964) 2588.
[7] D. Salomon, P.J. West, G. Weyer, Hyp. Int. 5 (1977) 61.
[8] D. Liljequist, USIP Report 80–07, 1980.
[9] H. Bethe, Ann. Phys. 5 (1930) 325.
[10] D.C. Joy, S. Luo, Scanning 11 (1989) 176.
[11] M.J. Berger, S.M. Seltzer, Nuclear Science Series Report #39, NAS-NRC (Natl. Acad. Sci), Publ. 1133, 1964, p. 205.
[12] D. Liljequist, J. Phys. D: Appl. Phys. 10 (1977) 1363.
[13] D. Liljequist, J. Phys. D: Appl. Phys. 11 (1978) 839.
[14] D. Liljequist, T. Ekdahl, U. Bäverstam, Nucl. Instr. and Meth. 155 (1978) 529.
[15] D. Liljequist, J. Phys. D: Appl. Phys. 16 (1983) 1567.
[16] D. Liljequist, J. Appl. Phys. 57 (1985) 657.
[17] D. Liljequist, M. Ismail, Phys. Rev. B 31 (1985) 4131.
[18] J.M. Fernandez-Varea, R. Mayol, D. Liljequist, F. Salvat, J. Phys.: Condens. Matter 5 (1993) 3593.
[19] M. Fernandez-Varea, D. Liljequist, S. Csillag, R. Räty, F. Salvat, Nucl. Instr. and Meth. B 108 (1996) 35.
[20] D. Liljequist, Nucl. Instr. and Meth. B 142 (1998) 295.
[21] D. Liljequist, Nucl. Instr. and Meth. B 174 (2001) 351.
[22] H. Niedrig, J. Appl. Phys. 53 (1982) R15.
[23] A. Vértes, I. Kiss, Nuclear Chemistry, Elsevier, Amsterdam, 1987.
[24] F.A. Deeney, P.S. McCarthy, Nucl. Instr. and Meth. 166 (1979) 491.
[25] Description of the IMSL Fortran Library. Available from: <http://www.vni.com/books/dod/pdf/FNLMathDescrip.html>.